

Supplementary Information

Immobilizing a Single DNA Molecule at the Apex of AFM Tips through Picking and Ligation

*Duckhoe Kim, Nak-Kwan Chung, Jung Sook Kim, and Joon Won Park**

Department of Chemistry

Pohang University of Science and Technology

Pohang 790-784, Republic of Korea

Phone: +82 54 279 2119

E-mail: jwpark@postech.ac.kr

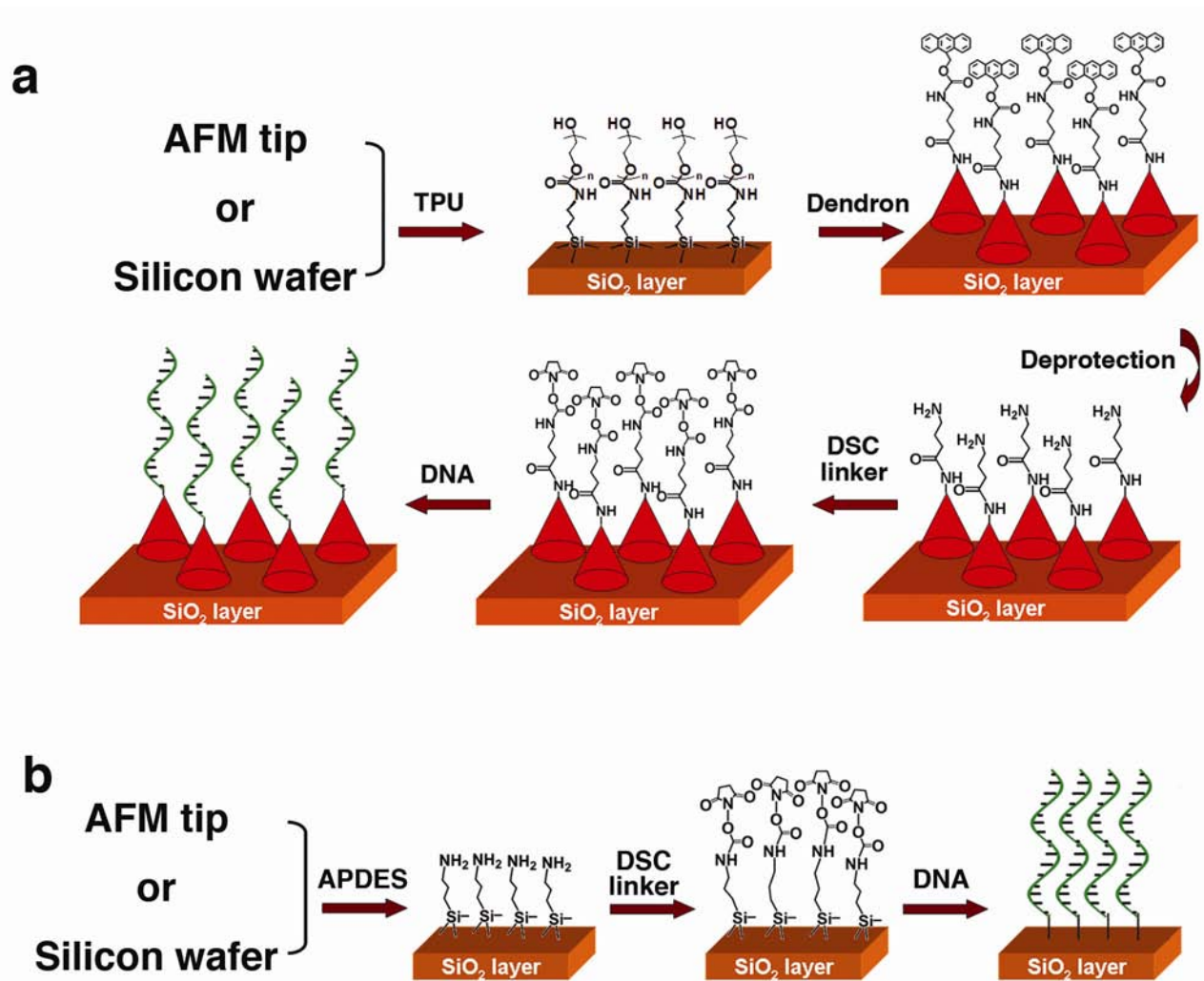


Figure S1. (a) Schematic diagram illustrating how to generate the dendron-modified substrate and AFM tip, and how to conjugate a DNA probe molecule to the dendron apex. (b) Schematic diagram showing treatment with APDES and the subsequent steps for the control experiments.

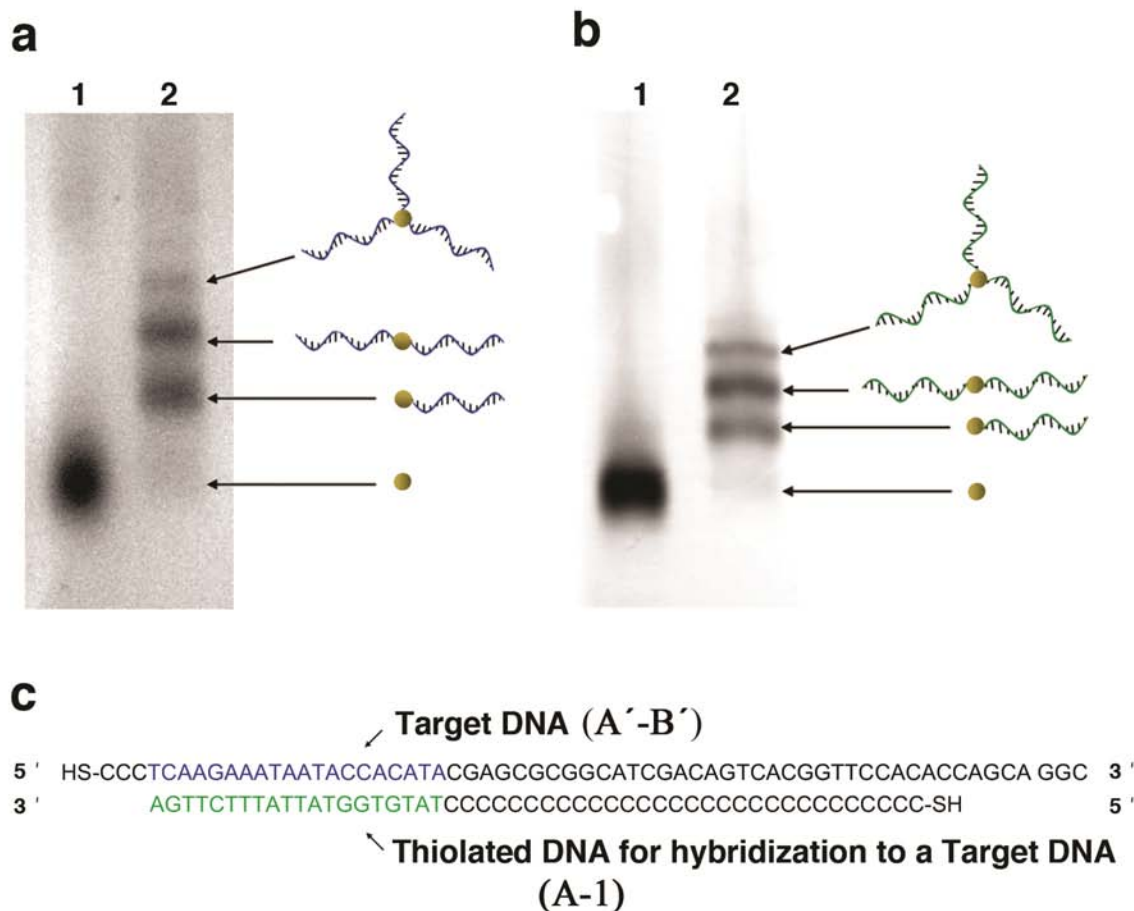


Figure S2. Isolation of AuNP-DNA conjugates with 3% agarose gel electrophoresis. (a) Gel image of the conjugate mixture. The phosphine-capped AuNPs were injected into column 1, and the various products were separated in column 2. (b) Gel image after conjugating the DNAs for the second hybridization with AuNPs. Reference materials were injected at column 1, and various isomers were separated in column 2. (c) Diagram showing the matching part of DNA used for the second hybridization.

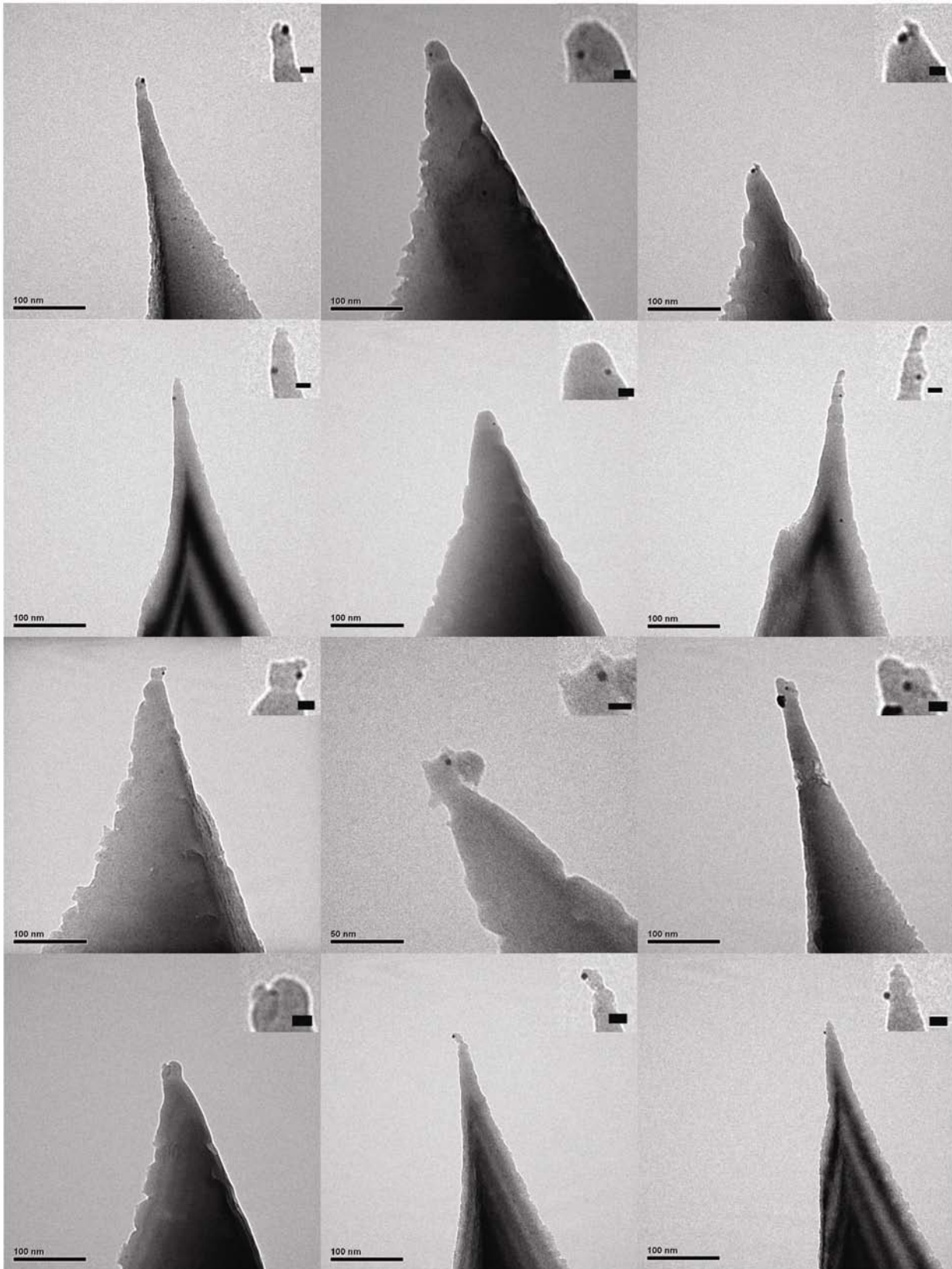


Figure S3. TEM images of additional AFM tips capturing a single target DNA molecule (inset scale bars, 10 nm). Picking was performed with five cycles at five different spots.

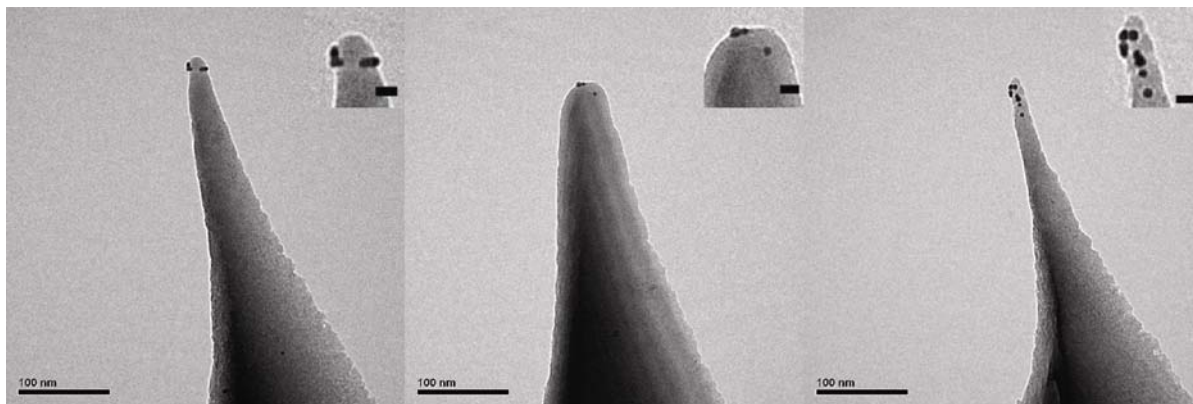


Figure S4. TEM images of AFM tips from the control experiments (inset scale bars, 10 nm).

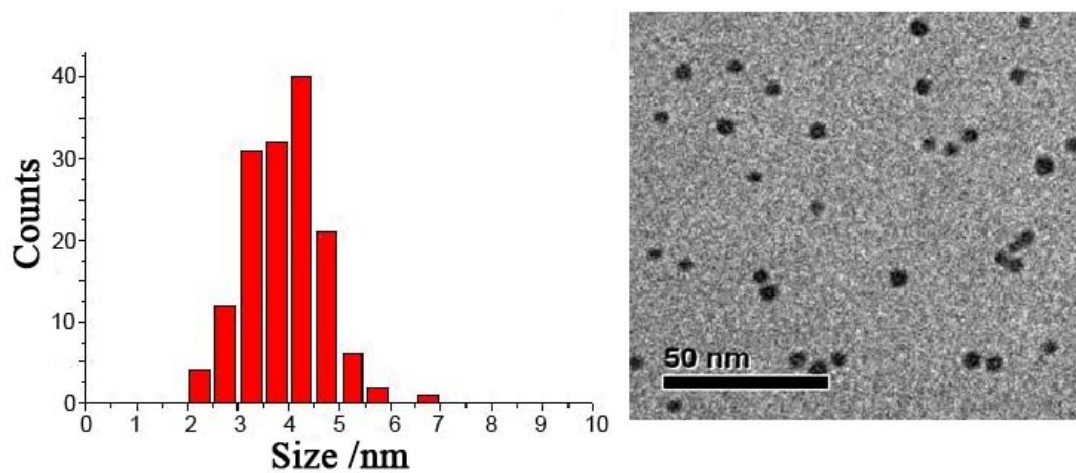


Figure S5. Histogram for the size of AuNPs which were used for the single DNA picking up. The diameter of each AuNP was obtained directly from TEM images of the AuNPs. As shown in the histogram and the TEM image, most of AuNPs were within 3 nm and 5 nm in diameter, and there were ones smaller than 3 nm (but no smaller than 2 nm) and ones larger than 5 nm (but no larger than 7 nm).

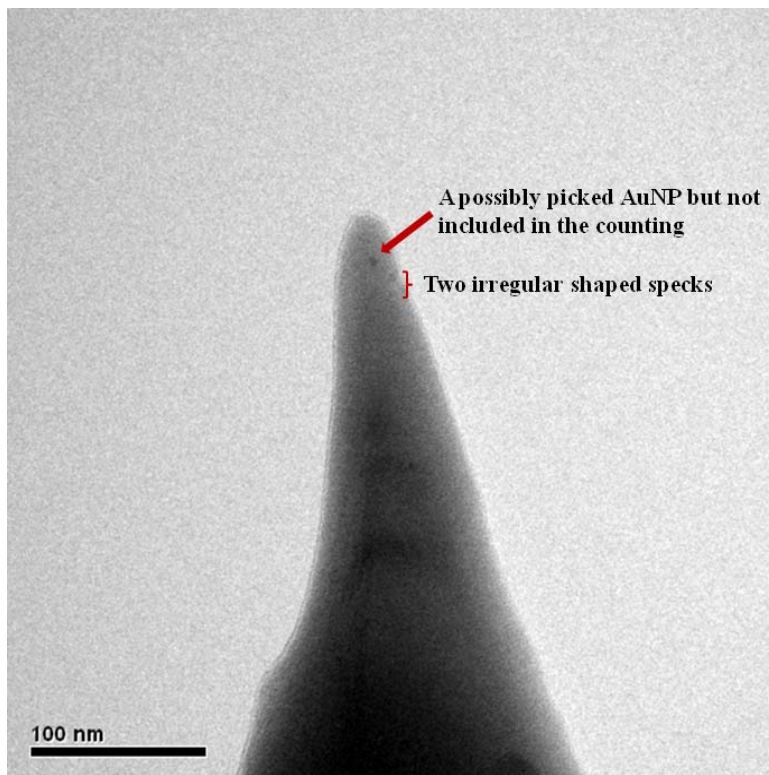


Figure S6. TEM image of a tip that shows a smaller particle. Because of the uncertainty, such cases were not included in counting the single DNA picking yield. Sometimes, tiny specks were also observed and revealed their irregular shapes upon adjusting the focal plane.

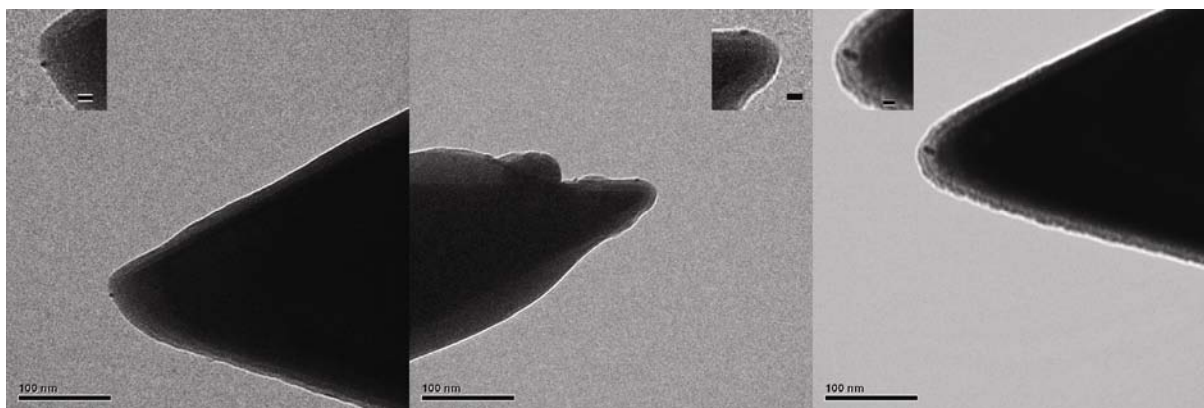


Figure S7. Influence of a larger tip radius was investigated. The tip velocity was fixed at $0.2 \mu\text{m/s}$, and the z-range was set to 500 nm. Five cycles were allowed at five different spots (a total of 25 cycles). While the yield was comparable, the tip picked either a single DNA (as in the left two images) or two DNAs (as in the right side image) (inset scale bars, 10 nm).

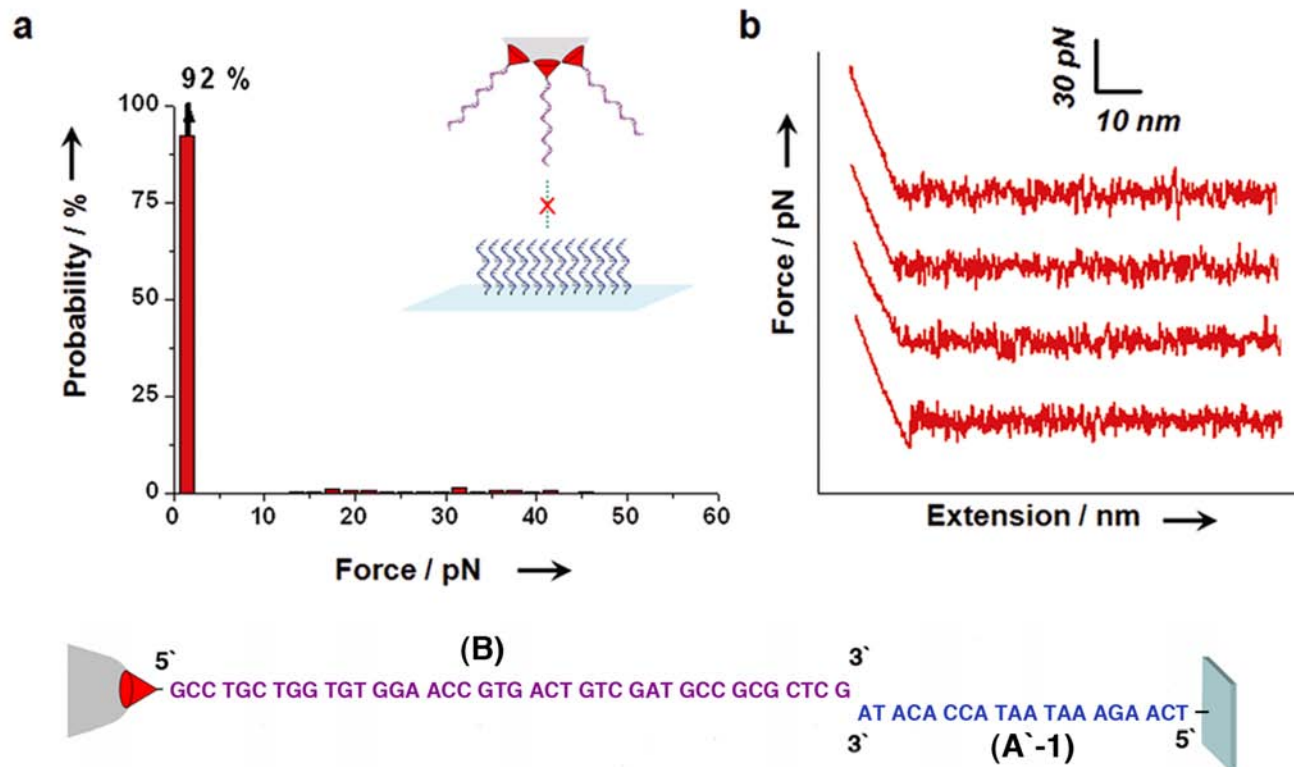


Figure S8. Interactions between the picker DNA only on the AFM tip (**B** in Table S1) and the 20-mer DNA (**A'-1** in Table S1), complementary to the 20-mer for the ligation (**A-2** in Table S1) (immobilized on the commercially available aldehyde-terminated slide). (a) Histogram of the unbinding force values recorded at a loading rate of $0.54 \mu\text{m sec}^{-1}$, (b) representative force-extension curves. 92% of no events were recorded. With the low frequency non-specific bindings were observed.

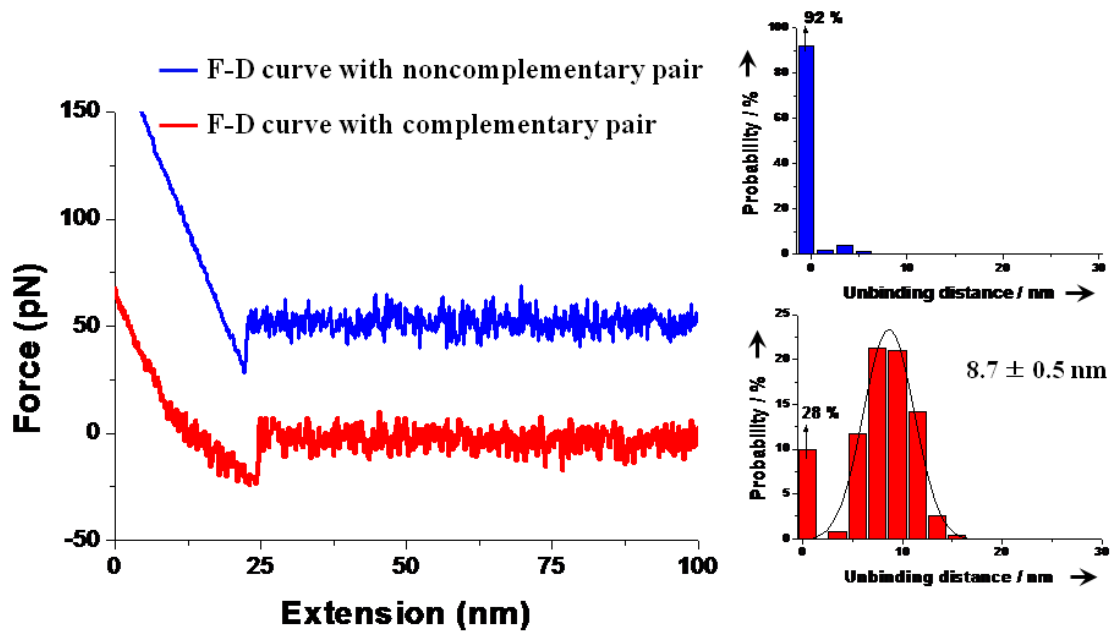


Figure S9. The stretching distance for the cases shown in Fig. 5 (complementary pair), and the corresponding histogram. While mostly no events and few nonspecific events characterized by the linear profile were observed for the noncomplementary pair, the complementary case showed a mean stretching distance of 8.7 ± 0.5 nm.

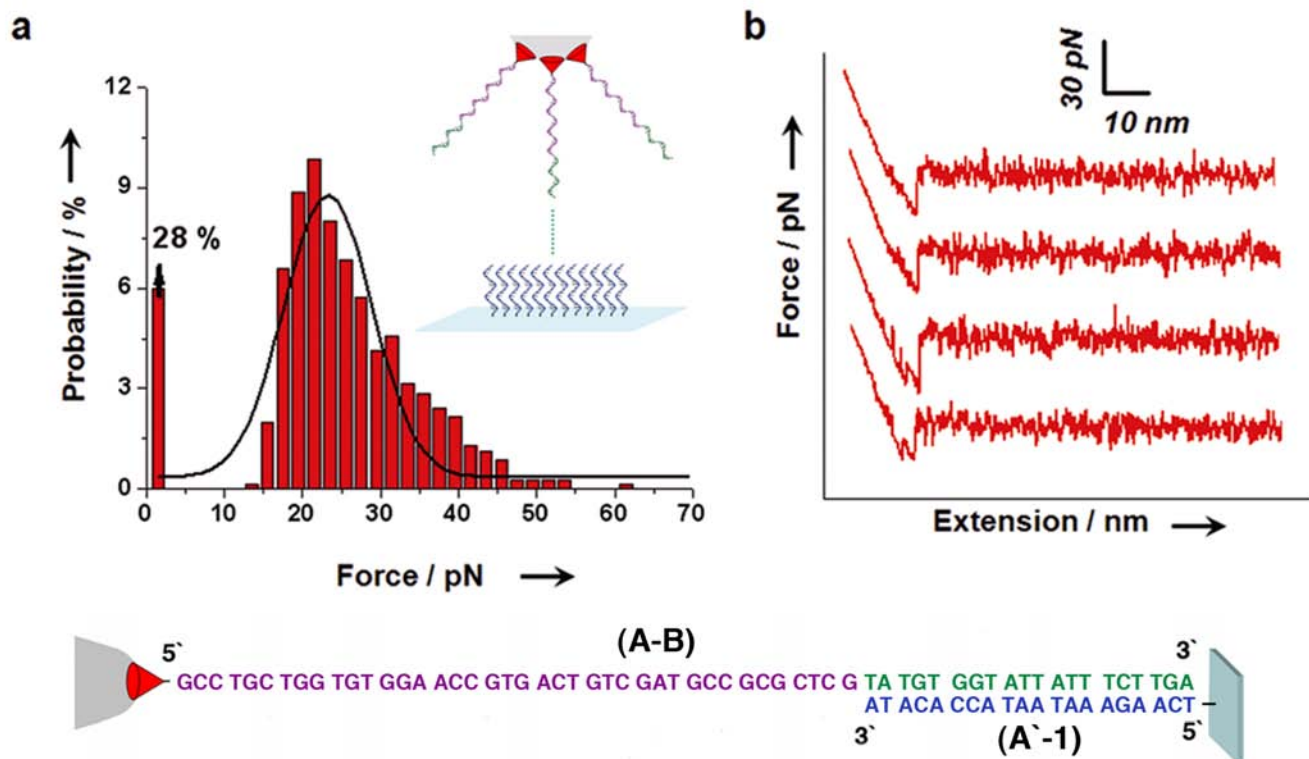


Figure S10. Interaction between the 60-mer DNA (**A-B** in Table S1) immobilized on the AFM tip and the 20-mer DNA (**A'-1** in Table S1) immobilized on the commercially available aldehyde-terminated slide. We immobilized the 60-mer DNA directly in solution phase for the control experiment. (a) Histogram of the unbinding force values recorded at a loading rate of $0.54 \mu\text{m sec}^{-1}$, (b) representative force-extension curves. Larger force values were recorded more frequently, and also double peaks were observed as shown in (b).

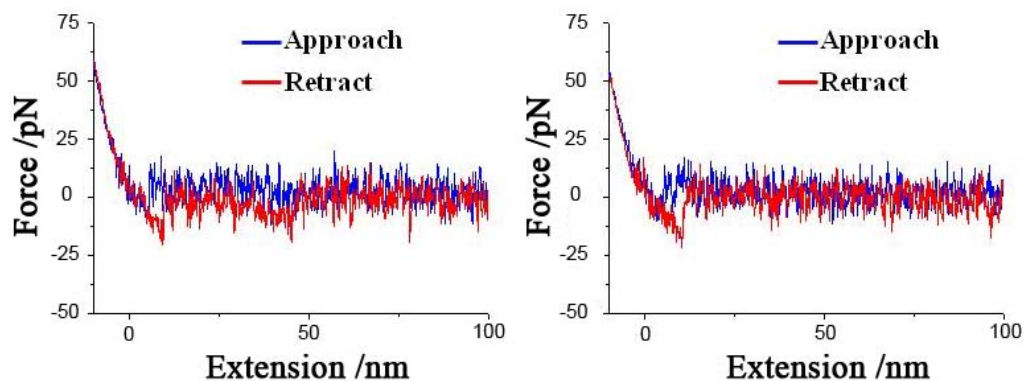


Figure S11. Two representative force curves for the specific DNA-DNA interactions (a pair of **A-2** and **A'-1** in Fig. 5). As evident, both binding (attractive) and unbinding (adhesive) events were observed with the complementary pair. In harmony with the previous report,^{S1} the binding force value was smaller than the unbinding force value at the retraction speed employed in this examination.

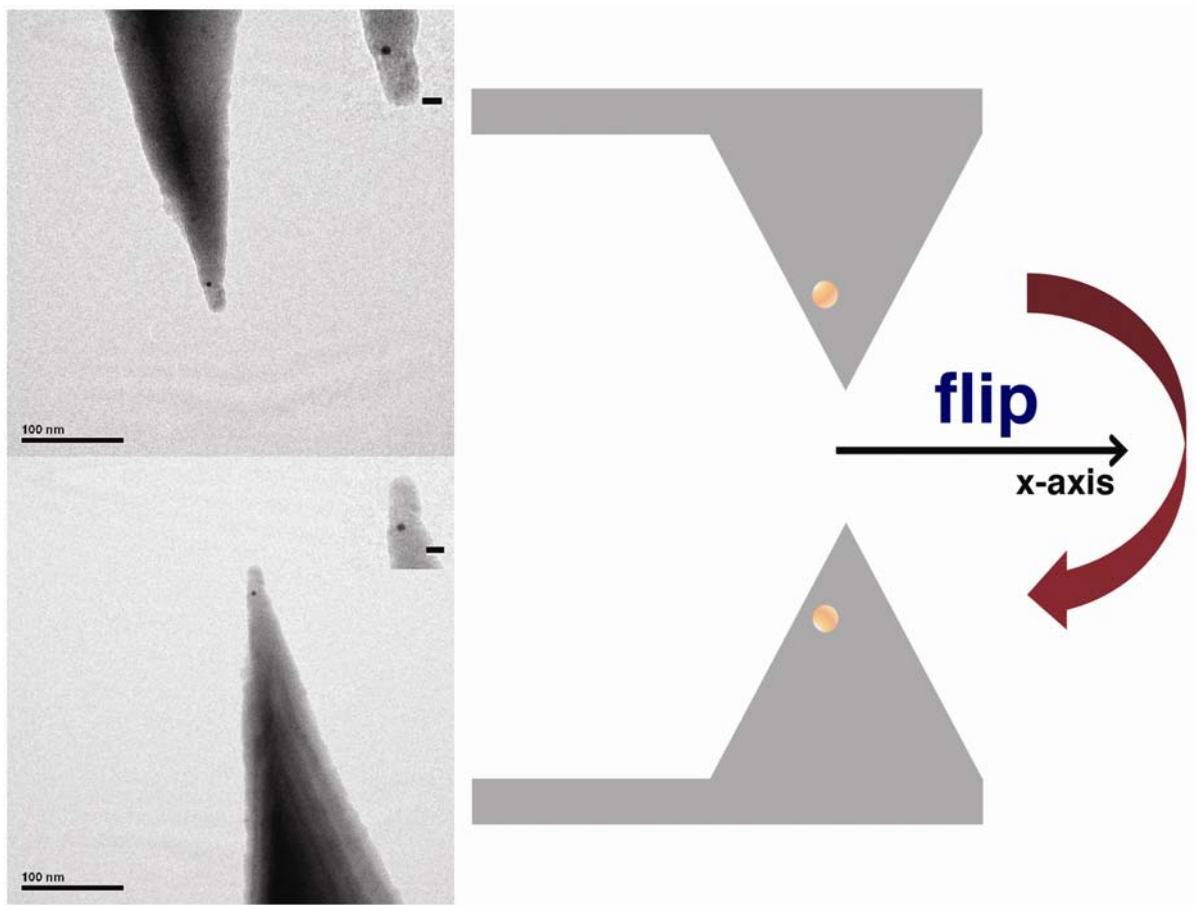


Figure S12. TEM images of an AFM tip before and after flipping around the x-axis (inset scale bars, 10 nm). After getting a TEM image of a tip, the tip was rotated 180° around the x-axis. A single AuNP was observed in both cases, and the position of the AuNP after flipping matched expectations.

Table S1. The sequence of DNAs used in this study.

	Sequence	Length
1. Probe DNA (A)	5'-TAT GTG GTA TTA TTT CTT GA CCC CCC CCC CCC CCC-(CH ₂) ₆ -NH ₂ -3'	35-mer
2. Target DNA (A'-B')	5'-SH-(CH ₂) ₆ CCC TCA AGA AAT AAT ACC ACA TAC GAG CGC GGC ATC GAC AGT CAC GGT TCC ACA CCA GCA GGC-3'	63-mer
3. Picker DNA (B)	5'-NH ₂ -(CH ₂) ₆ -GCC TGC TGG TGT GGA ACC GTG ACT GTC GAT GCC GCG CTC G-3'	40-mer
4. DNA for the second hybridization after the picking (A-1)	5'-SH-(CH ₂) ₆ -CCC CCC CCC CCC CCC CCC CCC CCC CCC CCC TAT GTG GTA TTA TTT CTT GA-3'	50-mer
5. DNA for the ligation (A-2)	5'-PO ₄ -TAT GTG GTA TTA TTT CTT GA-3'	20-mer
6. DNA immobilized on aldehyde slide for the force measurement (A'-1)	5'-NH ₂ -(CH ₂) ₆ -TCA AGA AAT AAT ACC ACA TA- 3'	20-mer
7. DNA that has both picker DNA and DNA for the ligation in tandem (A-B)	5'-NH ₂ -(CH ₂) ₆ -GCC TGC TGG TGT GGA ACC GTG ACT GTC GAT GCC GCG CTC GTA TGT GGT ATT ATT TCT TGA-3'	60-mer

Reference

- S1 Y. J. Jung, B. J. Hong, W. Zhang, S. J. B. Tandler, P. M. Williams, S. Allen and J. W. Park, *J. Am. Chem. Soc.*, 2007, **129**, 9349.